The published version is paper is available at https://doi.org/10.2514/1.J058334 1

Turbulent Heat Flux Model for Hypersonic Shock-Boundary Layer Interaction

Subhajit Roy[1] and Krishnendu Sinha[2]

Indian Institute of Technology Bombay, Mumbai 400076

Nomenclature

c_p	= Specific heat at constant pressure, J/kg.K
M	= Mach number
Pr_T	= Turbulent Prandtl number
q_w	= Wall heat flux, W/cm^2
r	= Mean density ratio
Re	= Reynolds number
$\overline{T}$	= Mean temperature, K
$\overline{u}$	= Mean velocity in x-direction, m/s
α_T	= Turbulent thermal diffusivity, m^2/s
δ_0	= Boundary layer thickness upstream of interaction, m
$\overline{\rho}$	= Mean density, kg/m^3
k	= Turbulent kinetic energy, m^2/s^2
ν_T	= Turbulent kinematic viscosity, m^2/s
ω	= Specific dissipation rate, s^{-1}

Subscripts

∞	= Free-stream condition
w	= Wall condition

---

[1] Doctoral student, Department of Aerospace Engineering. AIAA Member.
[2] Professor, Department of Aerospace Engineering. Senior AIAA Member.

I. Introduction

Predicting turbulent heat transfer in high-speed flows dominated by shock waves poses significant challenge to computational fluid dynamics (CFD) methods [1, 2]. The majority of the turbulence models are based on the gradient diffusion hypothesis, where the turbulent heat flux is modeled in terms of turbulent conductivity and turbulent Prandtl number (Pr_T). Conventional turbulence models in Reynolds-averaged Navier-Stokes simulations use a constant Pr_T value of 0.89; they often overpredict the wall heat transfer in shock-boundary layer interaction (SBLI). A few variable Pr_T models proposed in literature improve the heat flux prediction, but are computationally intensive [3, 4].

In a recent work, Quadros et al. [5] propose a new model for the turbulent heat flux based on the interaction of turbulent fluctuations with a normal shock [6]. The unsteady oscillations of an otherwise steady (in the mean) shock wave are found to have a dominant effect. It is modeled using the shock-unsteadiness model of Sinha et al. [7], which is based on linear interaction analysis of shock-turbulence interaction. The model is found to match DNS data for the peak turbulent heat flux generated by shock waves [5].

Roy et al. [8] cast the physics-based turbulent heat flux model in a variable Pr_T form, so as to readily integrate it into existing CFD codes. As per the new model, the turbulent Prandtl number is a function of the shock strength and the shock-unsteadiness parameter [7]. It takes a value lower than the conventionally accepted value of 0.89 and the value decreases for stronger shock waves. A lower Pr_T results in a higher turbulent conductivity and a higher turbulent heat flux than conventional models. More heat convected away from the wall by fluid turbulence leads to a lower peak heat transfer to the wall. The results match the peak heating measured in oblique shock boundary layer interaction for a range of shock strengths [9].

The primary advantage of the new variable Pr_T model is its algebraic form that makes it computationally efficient and numerically robust. It is applied in the region of shock waves and the model reverts back to the constant Pr_T version other wise. The model correction increases with the strength of the interaction, such that the significant improvements are obtained in predicting the peak heat transfer rate for strong shocks. In the limit of Mach 1, the model is calibrated to give vanishing small correction, so as to revert back to standard model in the absence of shock waves.

A limitation of the model is in the fact that it uses the shock-unsteadiness parameter for purely vortical turbulence upstream of the shock [7]. This is representative of low supersonic flow interacting with shock waves, where the thermodynamic fluctuations are expected to be small. This is not the case in hypersonic flows, where the temperature fluctuations can be appreciably large compared to the velocity fluctuations. In fact, the normalized rms temperature fluctuations scale with the square of the flow Mach number relative to the normalized rms velocity fluctuations, as per Morkovin's hypothesis [10].

In this paper, we extend the validity of the previous variable Pr_T model to high Mach number flows by including the effect of upstream temperature fluctuations. The shock-unsteadiness parameter in the previous version is replaced by its counterpart [11] that includes the effect of upstream temperature fluctuations. Otherwise, the earlier variable Pr_T framework is retained, so as to take advantage of its simple algebraic form and its computational efficiency. The new model is tested over a wide range of Mach numbers for different SBLI configurations. It shows significant improvement in hypersonic cases, while collapsing back to the earlier model for lower Mach numbers.

II. Model development

The current heat flux model for hypersonic flows builds upon the variable Pr_T model presented by Roy et al [8]. We describe the key steps in the development of the earlier model, which is based on the conservation of total enthalpy fluctuations across an unsteady oscillating shock wave.

$$T_1' + u_1' \frac{\bar{u}_1}{c_p} = T_2' + u_2' \frac{\bar{u}_2}{c_p} + \xi_t \frac{(\bar{u}_1 - \bar{u}_2)}{c_p} \tag{1}$$

where subscript 1 and 2 represent shock upstream and downstream locations and ξ_t is the unsteady shock speed. Overbar is used to denote mean quantities, while prime represents turbulent fluctuations.

The above equation is written by neglecting higher-order terms involving squares of velocity fluctuations, such that the left-hand side represents the total temperature fluctuations in the upstream of the shock. This can be taken to be zero, assuming that Morkovin's hypothesis [10] is valid in the incoming flow. Taking a moment of Eq. (1) with u_2' gives a relation for the downstream turbulent heat flux

$$c_p\overline{u'T'} = -\bar{u}\left(\overline{u'^2} + \overline{u'\xi_t}(r-1)\right) \tag{2}$$

where r is the mean density ratio across the shock and subscript 2 is dropped for convenience. The unclosed correlation between the shock speed and the velocity fluctuations is modeled in terms of the stream-wise Reynolds stress $\overline{u'\xi_t} = b_1\overline{u'^2}$, as per the shock-unsteadiness model of Sinha et al. [7].

We next convert Eq. (2) into an equivalent Pr_T formulation by evaluating the thermal diffusivity and eddy viscosity in terms of the turbulent transport in the shock-normal direction.

$$Pr_T = \frac{\nu_T}{\alpha_T} = \frac{3/4}{1 + b_1(r-1)} \tag{3}$$

The intermediate steps are delineated in section IV of Roy et al. [8], where it is argued that the normal shock analysis can be extended to the shock-normal direction of oblique shocks in SBLI flows. The above variable Pr_T model can be applied to any turbulence model. We choose the shock-unsteadiness k-ω model [12], which is known to improve separation prediction, and the associated surface pressure distribution in SBLI flows. The shock-unsteadiness parameter b_1 is obtained from linear interaction analysis [7], and is given by

$$b_1 = 0.4 + 0.6\left(\frac{6\psi - 1}{5\psi}\right)^{5.2} \tag{4}$$

where ψ is a shock function computed using the mean dilatation at a shock wave [8]. It is set to 1 in the undisturbed boundary layer and takes a value $1/r$ at shock waves.

The shock-unsteadiness model parameter b_1 corresponds to purely vortical turbulence upstream of the shock wave [7]. This limits the applicability of the model to supersonic flows up to Mach 5. For hypersonic flows, we need to account for additional fluctuations in the thermodynamic variables in the boundary layer upstream of the shock interaction. Morkovin's hypothesis [10] predicts that the temperature fluctuations in high-speed boundary layers are related to the velocity fluctuations as per

$$\frac{T'}{\bar{T}} = -(\gamma - 1)M^2\frac{u'}{\bar{u}} \tag{5}$$

Veera and Sinha [11] extend the original shock-unsteadiness model of Sinha et al. [7] to include the effect of upstream temperature fluctuations. They found that the shock-unsteadiness parameter is enhanced in the presence of temperature fluctuations, and is given by

$$b_1 = 0.4 + 0.6\left(\frac{6\psi - 1}{5\psi}\right)^{5.2} + 0.2(\gamma - 1)M_1^2 \tag{6}$$

The production of turbulent kinetic energy is also modified to include the effect of entropic production at shock waves. The model parameter b_1' in TKE equation is given by [11]

$$b_1' = \left[0.4 + 0.2(\gamma - 1)M_1^2\right]\left(\frac{1 - \psi}{5\psi}\right)^{0.3}. \tag{7}$$

We use the shock function ψ to compute the upstream shock-normal Mach number and it is used instead of local Mach number in the upstream boundary layer. This reduces the computational effort significantly and gives up to 10% error in the shock-unsteadiness parameters b_1 and b_1' for the present cases.

Otherwise, the implementation of the variable Pr_T model remains identical to that in [8]. In particular, the shock-detecting function f_s is computed using the boundary layer thickness δ_0 upstream of the interaction, and the values are is listed below. Also, Pr_T in Eq. (3) is used with a blending function ζ to transition smoothly to $Pr_T = 0.89$ in regions without shock waves. The sensitivity of the solution to the blending parameter χ is reported in [8] SBLI at Mach 5. At higher Mach numbers considered in this work, we find a lower sensitivity (less than 6%) of the wall heat flux to the variations in the blending parameter.

III. Results

The variable Pr_T model presented above is implemented in a Reynolds-averaged Navier Stokes code based on the k-ω framework. The k-ω model of Wilcox [13] is used as the baseline model and all the corrections are applied with respect to it. The shock-unsteadiness modified k-ω models of Sinha et al. [7] and of Veera and Sinha [11] are also used for turbulence closure. The models do not include any compressibility correction, as they are found to deteriorate model predictions in the undisturbed boundary layer upstream of the interaction [14, 15]. The finite volume formulation is identical to that used in the previous work [8], where the inviscid fluxes are computed using a low-dissipation Steger Warming flux splitting method [16]. The viscous fluxes and the turbulence source terms are computed via central difference. The code is second-order accurate in space, and

Table 1 The freestream and wall conditions in the SBLI experiments [18] and the computed boundary-layer thickness (δ_0) at upstream location x_{up}.

	Deflection angle	M_∞	ρ_∞ (kg/m^3)	T_∞ (K)	T_w (K)	Re_∞/m $\times 10^6$	δ_0 (mm)	x_{up} (m)	k_∞,10^{-3} (m^2.s^{-2})	ω_∞,10^4 (s^{-1})
	36°	11.3	0.0825	61.0	300.0	36.00	21.0	−0.2	8.50	1.70
	36°	8.20	0.4990	70.0	298.0	145.0	17.0	−0.2	1.31	1.38
Ramp	33°	8.10	0.4910	71.7	297.0	139.0	16.5	−0.2	1.37	1.38
	30°	8.30	0.5060	68.9	296.0	149.0	15.0	−0.2	1.27	1.38
	27°	8.20	0.5090	71.1	296.0	147.0	15.0	−0.2	1.30	1.41
	33°	8.21	0.0437	60.4	306.5	14.30	20.0	−0.1	5.00	0.54
Cone-	33°	7.18	0.0572	66.6	302.5	15.60	19.0	−0.1	3.90	0.50
flare	33°	6.17	0.0737	56.7	297.4	18.90	17.5	−0.1	1.97	0.40
	33°	5.10	0.2840	75.8	294.6	50.20	15.0	−0.1	0.69	0.38

uses the data parallel line relaxation method [17] for implicit time integration to reach steady state solution.

A. Compression ramp

We compute two-dimensional compression corner cases presented by Holden et al. [18], with a 1.02 m long plate followed by a 0.3 m ramp. A series of tests were conducted with the ramp angle varying between 27° and 36° at free stream Mach number around 8 and a 36° ramp at Mach 11.3 (table 1). The plate length is long enough to have a fully developed turbulent boundary layer upstream of the interaction [18]. This eliminates any potential uncertainty in the RANS computations due to laminar to turbulent transition. The highest temperature encountered in the simulations is around 850 K, thus justifying the perfect gas assumption employed in the governing equations. The wall temperature is reported for each case, and it is specified as an isothermal boundary condition, along with velocity no-slip, on the compression ramp. The boundary conditions on the turbulence variables are specified as per [19], where the length of the plate (1.02m) and cone

(2.35m) are taken as the characteristic lengths for calculating ω_∞ for the compression ramp and cone-flare cases. The computational domain extends from the tip of the plate to the end of the ramp, where an extrapolation condition is used at the flow exit boundary. The subsequent expansion is not simulated, as it is expected to have negligible effect on the surface properties in the interaction region.

The computational grid consists of 600×250 points, with exponential stretching in the wall-normal and wall-parallel directions. The first cell height is 1x10^{-6} m next to the wall, which is equivalent to 0.4 wall units or less along the compression ramp geometry. A rigorous grid refinement study is done for the strongest interaction at Mach 11.3, with three successively refined grids (400×150, 600×250 and 900×400) and the near wall spacing was reduced by a factor of 2 each time. The peak wall heat transfer showed a converging trend; the difference is less than 3% between the two finer meshes and the solutions are otherwise identical. Further refinement to 1300×600 grid points gives close to 1% variation in the peak heating rate.

Figure 1 shows the computed surface pressure and heat transfer rate for the strongest interaction at Mach 11.3. The results are compared with experimental data measured along the model center line, where three-dimensional effect are found to be negligible [18]. The pressure rise at $x = -0.08$ m corresponds to the separation point and it is well predicted by the current model (denoted by SU k-ω 2009) based on the shock-unsteadiness correction of Veera and Sinha [11]. The original shock-unsteadiness model (denoted by SU k-ω 2003) of Sinha et al. [7] over-predicts flow separation, because of excessive damping of turbulence kinetic energy at hypersonic Mach numbers. The baseline model suppresses flow separation, and results in a pressure rise close to the corner ($x = 0$). The current model matches the pressure plateau in the separation region, predicts a small peak at reattachment and overlaps with the pressure data measured on the ramp. The SU k-ω 2003 model also predicts a local pressure peak on the ramp, but its location is shifted downstream, because of a larger recirculation region.

The wall heat flux data (Fig. 1b) shows a modest increase at the separation point, and a steep rise at the corner. The present calculation using SU k-ω 2009 model, with variable Pr_T Eq. (3), reproduces the experimental measurements closely. It also matches the narrow peak in wall heat

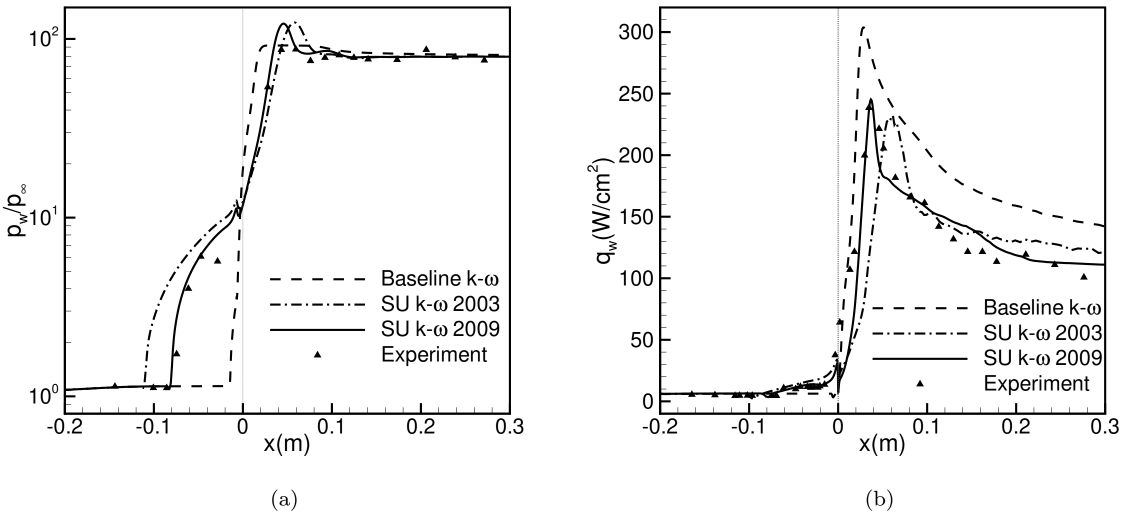

Fig. 1 Comparison of (a) surface pressure and (b) wall heat flux for 36^o **compression ramp at** $M_\infty = 11.3$ **using baseline and shock-unsteadiness modified** k-ω **models with the experimental data of Holden [18].**

flux near reattachment and the subsequent decrease in the surface heating rate on the ramp. The SU k-ω 2003 model, along with earlier variable Pr_T model [8], predicts a lower peak heat transfer rate and its location is shifted downstream compared to the experiment. The baseline k-ω model completely misses the separation bubble, and gives a single rise in heat flux at the corner. The wall heating is over predicted by 25-30 % along the entire ramp surface. It is important to predict the correct separation point and the size of the separation bubble, as it determines the strength of the separation shock and the resulting shock-shock interaction at reattachment [20]. This has a first-order effect on the peak heat transfer rate and its location on the ramp.

Figure 2 is a composite figure of all the Mach 8 compression corner cases, with the ramp angle varying from 36° to 27°, computed using SU k-ω 2009 model. The heat flux data plotted in Fig. 2b are normalized by the respective values at upstream location x_{up}; see table 1. The data is offset by 9, 23 and 36 units for the 30°, 33° and 36° cases, respectively, and the peak values are marked for easy comparison. Also the pressure axis is multiplied by a factor of 5, 30 and 100 for the 30°, 33° and 36° cases, respectively, and the normalized ramp pressure is noted in Fig. 2a.

As expected, the separation bubble size, identified by the pressure rise upstream of the corner, moves closer to the corner as the ramp angle decreases. The weakest interaction for the 27° ramp

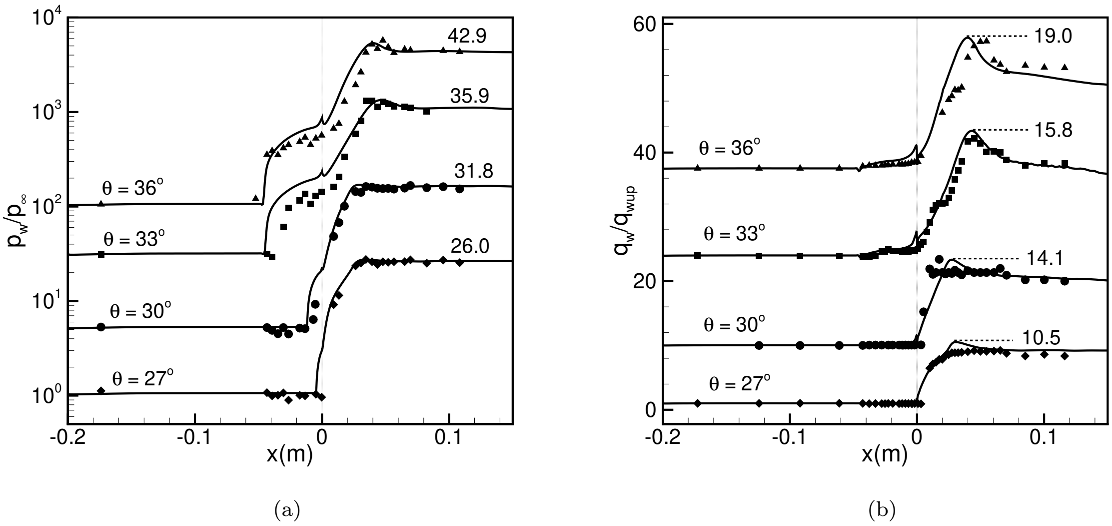

Fig. 2 Compression ramp (a) surface pressure and (b) wall heat flux for different deflection angles at $M_\infty \simeq 8$. Computations using SU k-ω 2009 model are compared with experimental data [18].

has incipient separation. The computations match the separation location well for all the cases, except the 33° interaction. The pressure plateau in the separation bubble is over-predicted, but the peak pressure and the ramp pressure are reproduced closely. A similar trend is observed for the wall heat transfer rate (Fig. 2b), where the current model matches the experimentally measured peak heat flux. The only exception is the 27° case, where the model overpredicts the heat transfer on the ramp. The location of the peak heat flux is reproduced correctly in the 33° SBLI, whereas it is predicted upstream and downstream of the experimental peak in the 36° and 30° cases respectively.

B. Cone-flare

Next, we consider the axisymmetric cone-flare configurations listed in table 1. The geometry consists of a 2.56 m long 7° half-angle cone and a 40° flare, which gives a 33° turning angle at the cone-flare junction. The computational domain extends from the tip of the cone to the end of the flare, and the outer boundary is tailored to the inviscid cone shock. The computational grid consists of 450×150 points, with fine grid at the cone tip and the cone-flare junction, and 90 points on the flare. Refining the grid to 850×250 points shows minimal changes in the solution, within 1.5% in the flare heat flux prediction for the strongest interaction at Mach 8.21. The first point next to the

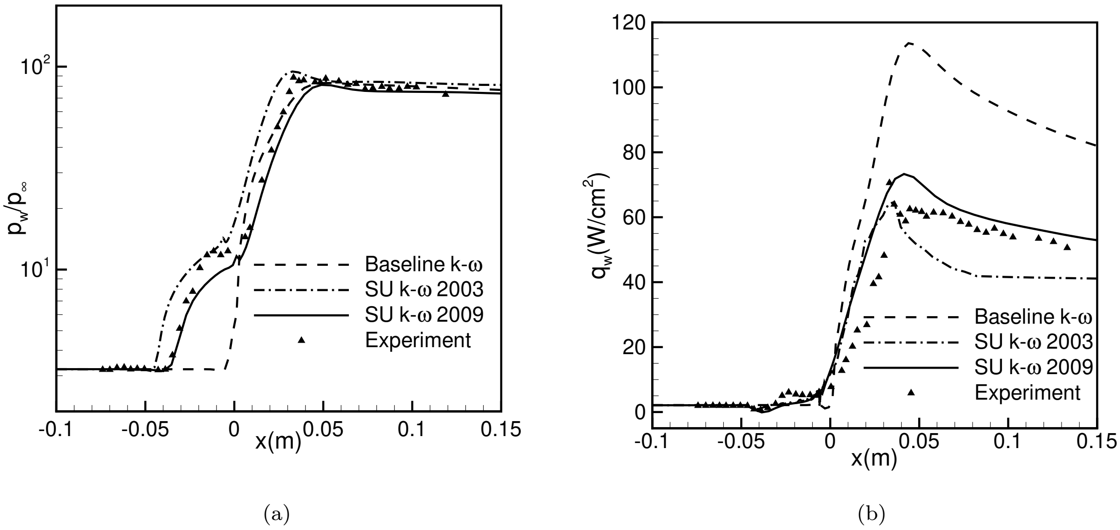

Fig. 3 Cone-flare (a) surface pressure and (b) wall heat flux predictions at $M_\infty = 8.21$ using baseline and shock-unsteadiness modified k-ω models compared with experimental data [18].

wall is placed at 10^{-6} m, which is equivalent to 0.5 wall units or less along the cone-flare surface.

The RANS equations are solved in axi-symmetric form, with the baseline, SU-2003 and SU-2009 forms of the k-ω model. The numerical method is identical to that described above and the boundary conditions are set as per the values listed in table 1. We follow the same steps as delineated for the compression ramp cases. In the absence of boundary layer profile measurements upstream of the interaction, we match the surface heat flux measurements on the cone within 7%. The flat plate heat flux data provided in the compression ramp cases is also reproduced within 12% by the computations. This is comparable to the measurement error reported in the experiments [18].

The results obtained for the strongest interaction for freestream Mach number of 8.21 is shown in Fig. 3. The surface pressure measurements follow the expected trend of separation pressure rise at $x = -0.04$ m and a subsequent reattachment pressure rise on the flare ($x > 0$). The current model based on SU k-ω 2009 matches the pressure data on the cone and at the separation location. The pressure plateau in the recirculation bubble is under-predicted, but the solution matches the data on the flare fairly well. We see marked improvement in the surface heat flux prediction (Fig. 3b), where the current model predictions are comparable to the experimental data on the flare. The maximum heat flux measured at $x = 0.03$ m is arguably matched by the computation, but the location is shifted downstream. The SU k-ω 2003 model, on the other hand, under-predicts the flare

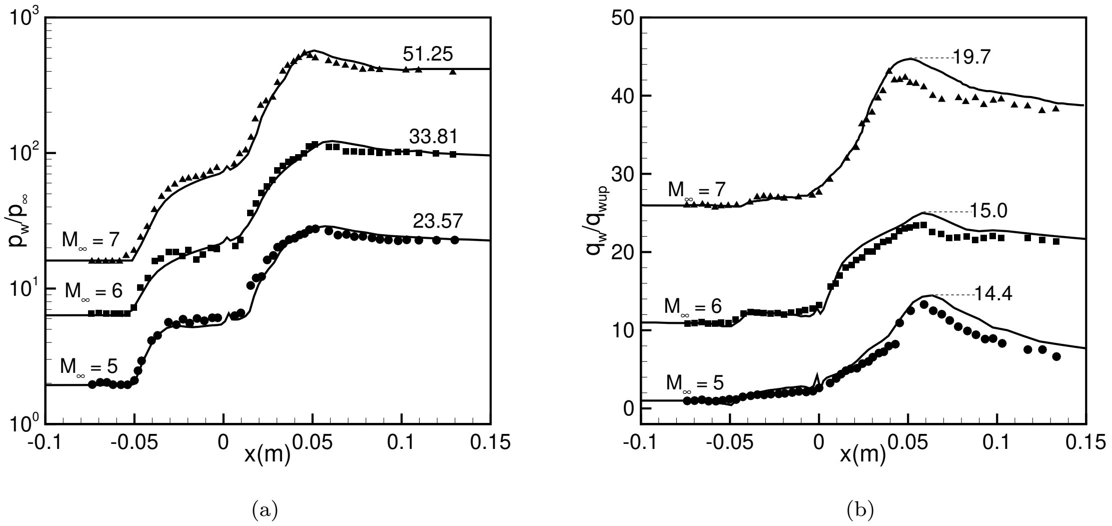

Fig. 4 Comparison of (a) surface pressure and (b) wall heat flux for cone-flare geometry at different Mach numbers with experiments [18].

heating rate, and the baseline k-ω model grossly over-predicts it. The separation location, in the pressure plot, is also not matched by the SU k-ω 2003 and baseline k-ω models, and the trends are similar to those observed for the compression ramp flow.

Figure 4 compares the SU k-ω 2009 surface predictions and the experimental measurements for the remaining cone-flare cases. Once again, the pressure data is scaled up for Mach 6 and 7 by factors of 3 and 8 respectively, while the heat flux is shifted up by 10 and 25 units respectively, compared to the Mach 5 case. The computations accurately reproduce the separation location for all the three flows. The pressure plateau in the separation bubble, the subsequent pressure rise at reattachment and the peak pressure on the flare also overlap with the experiments. The wall heat transfer data in Fig. 4b shows a reasonable match between the computed and measured values in the interaction region. The peak heat flux is over-predicted, but the trends in the computed solution follow the measurements on the wall. It is interesting to note that the separation location moves downstream as the Mach number increases. This is indicative of a smaller separation bubble and an earlier reattachment on the flare. As a result, the peak heat flux location moves upstream with increasing Mach number. The SU k-ω 2009 model predicts this trend and is thus physically consistent with the experimental observations.

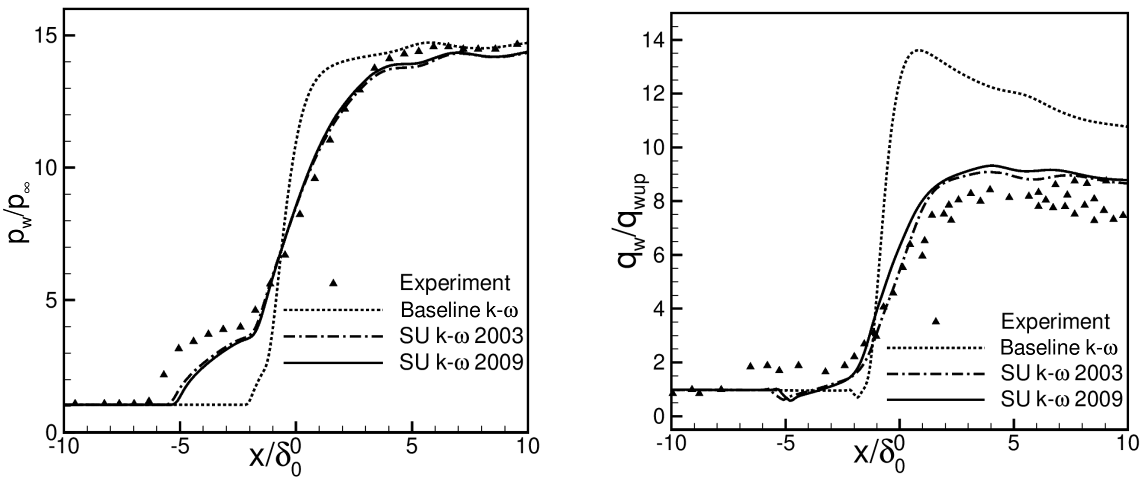

(a) (b)

Fig. 5 Oblique shock impingement at Mach 5: (a) surface pressure and (b) wall heat flux. Baseline and SU k-ω models are compared with the experimental data of Schulein [9].

C. Oblique shock impingement

We finally apply the SU k-ω 2009 model to the oblique shock impingement on a Mach 5 turbulent boundary layer. The experimental data is reported by Schulein [9] for a 14° shock generator angle and Reynolds number based on momentum thickness of 6982. This is one of three cases used for validating the variable Pr_T model based on SU k-ω 2003 in Roy et al. [8]. The full details of the SBLI configuration, computational grid and boundary conditions are given therein, and are not repeated here.

Figure 5 shows that the surface pressure and heat transfer rate are predicted well by the SU k-ω 2003 model, and the current SU k-ω 2009 model gives almost identical results. Specifically, both models predict the separation pressure rise downstream of the experiment, but match the subsequent pressure rise accurately. They also give significant improvement in predicting the reattachment wall heat flux compared to baseline k-ω model.

The important point is that there is less than 5% difference between the two models, and the same is true for the other Mach 5 oblique shock impingement cases reported by Schulein [9]. In fact, the current model is expected to collapse to the earlier Pr_T model [8] for Mach numbers below 5. This is because of the fact that the extra term $(\gamma - 1)M^2$ in Eq. (6) has a negligible contribution in non-hypersonic boundary layers, where $1 < M < 2$ in the log layer. As noted in our earlier work [21], the log-layer value of the turbulent Prandtl number is critical in predicting the wall heat flux accurately.

IV. Conclusion

In this paper, we develop a variable turbulent Prandtl number model for predicting the wall heat transfer in hypersonic shock-boundary layer interaction. It is an extension of an earlier model based on the physics of unsteady shock motion in a turbulent flow. It uses the shock-unsteadiness parameter for flows with upstream temperature fluctuations typical of hypersonic turbulent boundary layers. The new model is found to predict the peak heat transfer consistently over a range of Mach numbers and geometric configurations. It also matches the experimentally observed separation location, and gets physically consistent results with varying shock strength. Finally, the model collapses to the earlier version that has been thoroughly tested for SBLI at lower Mach numbers.

References

[1] Bose, D., Brown, J.L., Prabhu, D.K., Gnoffo, P., Johnston, C.O., and Hollis, B., "Uncertainty assessment of hypersonic aerothermodynamics prediction capability," *Journal of Spacecraft and Rockets*, Vol. 50, No. 1, 2013, pp. 12-18. DOI: 10.2514/1.A32268

[2] Gnoffo, P. A., Berry, S.A., and Norman, J.W.V., "Uncertainty assessments of hypersonic shock wave-turbulent boundary-layer interactions at compression corners," *Journal of Spacecraft and Rockets* Vol. 50, No. 1, 2013, pp. 69-95. DOI: 10.2514/1.A32250

[3] Xiao, X., Edwards J.R., Hassan A. H., and Gaffney R.L., "Role of turbulent Prandtl numbers on heat flux at hypersonic Mach numbers," *AIAA Journal*, Vol. 45, No. 4, 2007, pp. 806-813. DOI: 10.2514/1.21447

[4] Ott, J.D., Donald C.K., and Dash, S.M., "Evaluation of Turbulence Modeling Extensions for the Analysis of Hypersonic Shock Wave Boundary Layer Interactions," *51st AIAA Aerospace Sciences Meeting Including the New Horizons Forum and Aerospace Exposition*, AIAA Paper 2013-0983, Jan. 2013. DOI: 10.2514/6.2013-983

[5] Quadros, R. and Sinha, K., " Modelling of turbulent energy flux in canonical shock-turbulence interaction," *International Journal of Heat and Fluid Flow*, Vol. 61, 2016, pp. 626-635. DOI: 10.1016/j.ijheatfluidflow.2016.07.006

[6] Quadros, R., Sinha K. and Larsson J., "Turbulent energy flux generated by shock/homogeneous-turbulence interaction," *Journal of Fluid Mechanics*, Vol. 796, June 2016, pp. 113-157. DOI:10.1017/jfm.2016.236

[7] Sinha, K., Mahesh K., and Candler, G.V., "Modeling shock unsteadiness in shock/turbulence interaction," *Physics of Fluids*, Vol.15, No. 8, 2003, pp. 2290-2297. DOI: 10.1063/1.1588306

[8] Roy, S., Pathak, U. and Sinha, K., "Variable Turbulent Prandtl Number Model for Shock/Boundary-Layer Interaction," *AIAA Journal*, Vol. 56, No.1, 2018, pp. 342-355. DOI: 10.2514/1.J056183

[9] Schulein, E., "Skin friction and heat flux measurements in shock/boundary layer interaction flows," *AIAA Journal*, Vol. 44, No. 8, 2006, pp. 1732-1742. DOI: 10.2514/1.15110

[10] Morkovin, M.V., "Effects of compressibility on turbulent flows," *Mecanique de la Turbulence*,edited by A. Favre, Gordon and Breach, New York, 1964, pp. 367-380.

[11] Veera, V.K., and Sinha, K., "Modeling the effect of upstream temperature fluctuations on shock/homogeneous turbulence interaction," *Physics of fluids*, Vol. 21, No. 2,2009, pp. 1-10. DOI:10.1063/1.3073744

[12] Sinha, K., Mahesh K., and Candler, G.V., "Modeling the effect of shock unsteadiness in shock/turbulent boundary-layer interactions," *AIAA Journal*, Vol. 43, No. 3, 2005, pp. 586-594. DOI: 10.2514/1.8611

[13] Wilcox, D.C., "Turbulence modeling for CFD." 1^{st} ed., La Canada, CA: DCW industries, 1993.

[14] Forsythe, J., Hoffmann, K., and Damevin, H.M., "An assessment of several turbulence models for supersonic compression ramp flow," 29th AIAA, *Fluid Dynamics Conference*, AIAA Paper 1998-2648, Albuquerque, New Mexico 15-18 June 1998. DOI: 10.2514/6.1998-2648

[15] Coakley, T., and Huang, P., "Turbulence modeling for high speed flows," *30th Aerospace Sciences Meeting and Exhibit*, AIAA Paper 1992-436, Reno, Nevada 6-9 January 1992. DOI: 10.2514/6.1992-436

[16] MacCormack, R.W., and Candler, G.V., "The solution of the Navier-Stokes equations using Gauss-Seidel line relaxation," *Computers & fluids*, Vol. 17, No. 1, 1989, pp. 135-150. DOI: 10.1016/0045-7930(89)90012-1

[17] Wright, M.J., Candler, G.V, and Bose, D., "Data-parallel line relaxation method for the Navier-Stokes equations," *AIAA Journal*, Vol. 36, No. 9, 1998, pp. 1603-1609. DOI: 10.2514/2.586

[18] Holden, M. S., Wadhams, T., MacLean, M., and Dufrene, A., "Measurements in Regions of Shock Wave/Turbulent Boundary Layer Interaction from Mach 4 to 10 for Open and Blind Code Evaluation/Validation," 21st AIAA *Computational Fluid Dynamics Conference*, AIAA Paper 2013-2836, San Diego, California 24-27 June 2013. DOI: 10.2514/6.2013-2836

[19] Menter, F.R., "Two-equation eddy-viscosity turbulence models for engineering applications," *AIAA*

Journal, Vol. 32, No. 8, 1994, pp. 1598-1605. DOI: 10.2514/3.12149

[20] Pasha, A.A., and Sinha, K., "Simulation of hypersonic shock/turbulent boundary-layer interactions using shock-unsteadiness model," *Journal of Propulsion and Power*, Vol. 28, No. 1, 2012, pp. 46-60. DOI: 10.2514/1.B34191

[21] Pathak, U., Roy, S., and Sinha, K., "A phenomenological model for turbulent heat flux in high-speed flows with shock-induced flow separation," *Journal of Fluids Engineering*, Vol. 140, No. 5, 2018, pp. 1-9. DOI: 10.1115/1.4038760